

Brief Reports

Brief Reports are accounts of completed research which, while meeting the usual Physical Review standards of scientific quality, do not warrant regular articles. A Brief Report may be no longer than four printed pages and must be accompanied by an abstract. The same publication schedule as for regular articles is followed, and page proofs are sent to authors.

Iron at high pressure: Linearized-augmented-plane-wave computations in the generalized-gradient approximation

Lars Stixrude

School of Earth & Atmospheric Sciences, Georgia Institute of Technology, Atlanta, Georgia 30332-0340

R. E. Cohen

Geophysical Laboratory and Center for High Pressure Research, Carnegie Institution of Washington, 5251 Broad Branch Road N.W., Washington, D.C. 20015-1305

D. J. Singh

Complex Systems Theory Branch, Naval Research Laboratory, Washington, D.C. 20375-5345

(Received 3 November 1993)

General potential linearized-augmented-plane-wave computations using the generalized-gradient approximation (GGA) of Perdew and Wang (PW-II) show excellent agreement with the measured equations of state of bcc and hcp phases to over 300 GPa, the bcc to hcp phase transition pressure, and the bcc magnetic moment. The results are a significant improvement over the local-spin-density approximation and the earlier PW-I GGA functional. The bcc phase is mechanically unstable at high pressure with respect to a tetragonal strain, and is thus unlikely to exist in the earth's inner core.

The phase diagram of iron at very high pressure and temperature is of considerable geophysical interest because the earth's liquid outer core and solid inner core are composed primarily of this element. Thermal and compositional models of the core and the overlying mantle, which receives much of its heat from the core, are strongly dependent on our knowledge of the phase stability of iron and its alloys.¹ The melting curve of iron constrains the geotherm at the inner core-outer core boundary near the center of the earth (5150 km depth or 329 GPa). The subsolidus phase diagram at higher pressures (329–364 GPa) determines the crystalline structure and physical properties of the inner core, including the as yet unexplained elastic anisotropy of this region.² The continued growth of the inner core, by freezing of the overlying outer core, is a major energy source in the earth's interior and is primarily responsible for the fluid motions which produce the geomagnetic field.³ Despite recent experimental progress toward measuring the iron melting curve by both static^{4–6} and dynamic^{4,7} techniques, and the possible discovery of a new, as yet uncharacterized, high-pressure phase,^{5,6} the phase diagram of iron is still highly uncertain at extreme pressures and the crystalline structure of the inner core remains essentially unknown. To better understand the physics of solid iron and to place constraints on its phase stability under core conditions, we have performed first-principles density-functional calculations of bcc, fcc, and hcp phases en-

compassing the entire pressure range of the earth.

Density-functional theory yields exact ground-state properties in principle. However, the exact exchange-correlation energy functionals are unknown. The most widely used approximation, the local-density approximation (LDA), has enjoyed considerable success. It is not universally successful however. Among its deficiencies in condensed-matter applications are overestimated binding energies and bulk moduli and underestimated volumes of 3d solids.⁸ Of its most widely studied shortcomings is the incorrect prediction of a close-packed nonmagnetic ground state for iron rather than the ferromagnetic bcc structure.⁹

There have been many attempts to go beyond the LDA. A Taylor-series expansion in the charge-density gradient, of which the LDA represents the first term, yields poor results because leading-order terms violate the sum rules for the exchange-correlation hole which LDA satisfies.¹⁰ Generalized-gradient approximations (GGA's) go beyond the LDA while maintaining the sum rules which appear central to its success.^{11–13} Among the most widely used are those of Perdew and Wang [PW-I (Ref. 12), PW-II (Ref. 13)]. PW-II is based on an entirely real-space analysis of the fluctuation hole cutoffs, treating exchange and correlation functionals on an equal footing. It also obeys known bounds and limits on the exchange functional.^{14,15}

The relative energies and equations of state of the

phases of iron represent an important test of gradient-corrected functionals. It is well known that the Langreth-Mehl and Perdew-Wang functionals predict ferromagnetic bcc to be more stable than fcc iron.^{16–22} However, the global ground state of these functionals for iron is not well established, since most studies have not considered the hcp structure. The energetics of the hcp structure in GGA is an important issue for several reasons. First, predictions can be compared with experimental observations of the bcc to hcp phase transition,²³ which provides a stringent test of the predicted energy difference between these two phases. Second, since hcp is nonmagnetic, the bcc-hcp energy difference tests the degree of magnetic stabilization in GGA. Third, measurements of the hcp equation of state to more than 3 Mbar (300 GPa)²⁴ provide an opportunity to compare theory and experiment over a nearly twofold range of compression.

We investigated the energetics of bcc, fcc, and hcp structures with the PW-II functional using the general potential linearized-augmented plane-wave (LAPW) method.²⁵ The LAPW method is free of shape approximations to the charge density or the potential. This is significant because shape approximations such as the muffin-tin or the atomic-sphere approximation (ASA)^{15–17,20,22} have been shown to result in errors in the bcc-fcc energy difference of approximately 4 mRy, comparable to the energy difference itself.^{17,19} The only previous investigation of the hcp structure using gradient-corrected functionals used the LMTO-ASA method and assumed the ideal hcp structure.²¹ Here we investigate distortions of the hcp lattice away from the ideal c/a ratio since this is a source of energy potentially comparable to the small bcc-hcp energy difference.

Explicit forms for the PW-II functional appear in Ref. 13. The form of von Barth and Hedin²⁶ was adopted for local-spin-density approximation (LSDA) calculations. Ferromagnetic bcc and nonmagnetic bcc, fcc, and hcp structures are investigated over a range of atomic volumes, $V=40–90$ a.u. We focused on nonmagnetic fcc and hcp states since these are more stable than the corresponding magnetic states at nonnegative static pres-

ures.^{9,21,22} Lattice distortions of hcp and cubic structures are investigated by varying the c/a ratio. Core states are treated self-consistently using the full Dirac equation for the spherical part of the potential, while valence states are treated in the semirelativistic approximation which neglects spin-orbit coupling. $3s$, $3p$, $3d$, $4s$, and $4p$ electrons were treated as valence bands for all volumes. To eliminate problems with Fe p -like ghost states, the LAPW basis set was augmented with extra local functions so that a single energy window can accurately treat all the band states.²⁷ The local orbital extension eliminates linearization errors in the Fe d bands and potential problems due to nonorthogonality to the upper core states when small muffin-tin spheres needed for high-pressure studies are used.

We used a $16 \times 16 \times 16$ special k -point mesh,²⁸ yielding 140, 408, and 240 k points in the irreducible wedge of the Brillouin zone for bcc, fcc, and hcp structures, respectively, and a $12 \times 12 \times 12$ mesh (159 points) for tetragonally strained bcc states. The product of the muffin-tin radius, R_{MT} and the maximum reciprocal space vector, $R_{MT}K_{max}$ was set to 9.0 for tetragonally strained bcc calculations and 10.0 for the other structures. For $V=50–90$ a.u., $R_{MT}=2.0$ a.u. and from $V=40–60$ a.u., $R_{MT}=1.86$ a.u. and 1.83 a.u. for GGA and LSDA calculations, respectively. Careful convergence tests showed that, with these computational parameters, relative energies are converged to better than a few tenths of a mRy and magnetic moments to better than $0.05\mu/\mu_B$.

Binding energy curves show that PW-II correctly predicts the ferromagnetic bcc structure as the ground state (Table I, Fig. 1). We find, in agreement with previous results, that bcc is more stable than fcc.^{16–22} We also find that bcc is more stable than hcp, calculated to be the minimum energy close-packed structure at all volumes, in agreement with high-pressure experiments.²⁴ The gain in energy due to distortion of the hcp lattice is non-negligible (1 mRy) although even ideal hcp is more stable than fcc in both LSDA and PW-II at all volumes. The minimum energy c/a ratio (ranging from 1.58 at 0 GPa to 1.60 at 400 GPa) agrees well with experiment.²⁴ The slope of the common tangent to the bcc and hcp binding energy curves yields the equilibrium phase transition pressure. We find this to be 11 GPa in PW-II, in excellent agreement with experiments,²³ which show significant hysteresis but bracket the transition between 10 and 15 GPa. The properties of the transition are very similar to those found in LMTO-ASA calculations with the PW-I functional.²¹

Equations of state in the PW-II approximation show substantial improvement over LSDA. The equilibrium volume and bulk modulus of bcc differ from experiment by 3 and 9% respectively, compared with 12 and 35% discrepancies for LSDA. Similarly good agreement has been found before for PW-I (Refs. 16–19, 21, and 22) and PW-II (Ref. 20) functionals, although the two approximations give somewhat different results. In contrast to PW-II, PW-I overcorrects for the shortcomings of LSDA, producing an overexpanded equilibrium bcc lattice and bulk modulus somewhat smaller than observed. Incorporation of zero-point and thermal contributions,

TABLE I. Equation-of-state parameters determined by fitting an Eulerian finite strain expression (Ref. 32) to the computed binding energy curves. Experimental data from Ref. 23 (V_0, K_0 , zero-pressure volume, and bulk modulus, respectively) and Ref. 33 (K'_0 , pressure derivative of the bulk modulus).

		E_0 (Ry)	V_0 (bohr ³)	K_0 (GPa)	K'_0
Bcc	LSDA	-2541.0948	70.73	245	4.6
	GGA	-2546.3001	76.84	189	4.9
	Expt.		79.51	172	5.0
Fcc	LSDA	-2541.0988	65.06	340	4.4
	GGA	-2546.2890	69.32	288	4.4
Hcp	LSDA	-2541.1046	64.74	344	4.4
	GGA	-2546.2947	68.86	291	4.4

which have been neglected here, would further improve agreement between PW-II and experiment while degrading the comparison for PW-I. The significant differences between the two PW approximations suggests that a systematic investigation of transition metals with the more recent functional may be desirable. The pressure-volume relations are in good agreement over the measured pressure range. GGA pressure-volume curves differ from experiment by less than 3% for bcc and 1% for hcp at the highest experimental pressures (Fig. 2).

PW-II and LSDA yield very similar results for the magnetic moment of bcc over the entire volume range (within $0.2\mu_B$, Fig. 2). This is consistent with previous results over more limited ranges of volume.²⁰ At their equilibrium lattice constants, the two methods yield 2.174 and $2.044\mu_B$, respectively, approximately 3% smaller than LMTO results,²⁰ and in excellent agreement with the experimental value ($2.12\mu_B$). Both PW-II and LSDA show a vanishing moment at the highest pressures (Fig. 2).

Our results support a general pattern in which gradient-corrected functionals predict larger lattice parameters and stabilize magnetic structures relative to LSDA. The magnetic stabilization does not originate in

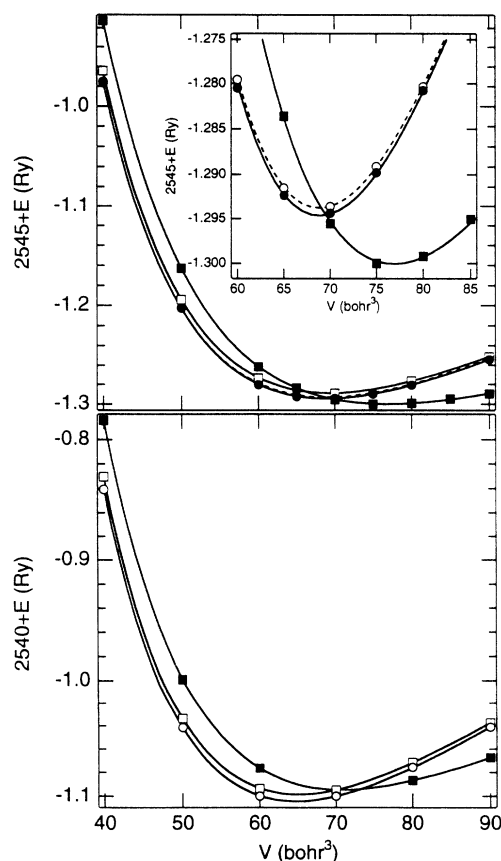


FIG. 1. Total energy vs volume in GGA (top) and LSDA (bottom) for bcc (solid squares), fcc (open squares) ideal hcp (open circles), and distorted hcp (solid circles). Inset: bcc to hcp transition region in GGA. For LSDA, only ideal hcp calculations were performed.

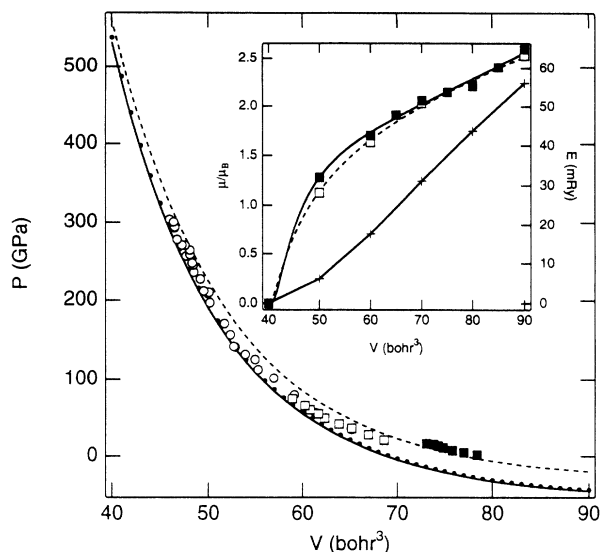


FIG. 2. GGA pressure-volume relations for bcc (dashed line), fcc (dotted line), and hcp (solid line). Hcp data: open circles (Ref. 24) and open squares (Ref. 23), bcc data: solid squares (Ref. 23). Inset: magnetic moment of bcc in GGA (solid squares, solid line) and LSDA (open squares, dashed line), and the GGA magnetic stabilization energy (crosses; nonmagnetic-ferromagnetic).

a larger magnetic moment, since PW-II and LSDA predict similar moments at all volumes. In the case of iron, the magnetic stabilization energy for PW-II (Fig. 2) is essentially that required to reproduce the observed bcc-hcp transition pressure. This shows that *overstabilization* of magnetic structures is not a general feature of PW functionals. Evidence for over-stabilization comes from calculations on Fe_3Ni with PW-I,²⁹ where the magnetic stabilization energy is found to be too large to permit the

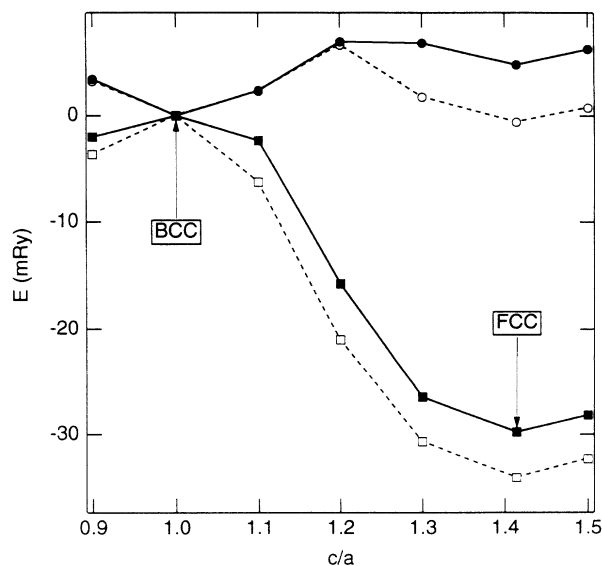


FIG. 3. Energy vs c/a ratio for Fe for GGA (solid curves) and LSDA (dashed) at two volumes, 70 a.u. (upper curves) and 50 a.u. (lower curves). The c/a ratios of the bcc and fcc structures are indicated.

standard explanation of the invar effect in terms of nearly degenerate low- and high-spin states. Other evidence comes from calculations on Cr which show that PW-II correctly predicts an antiferromagnetic ground state, unlike LSDA or Langreth-Mehl GGA functionals, but overestimates the magnetic moment.³⁰ However, this issue is complicated by the fact that the observed ground state of Cr is an incommensurate spin-density wave. We believe it significant that our results, which argue against magnetic overstabilization, are based essentially on ground-state energies and that they suggest a more extensive investigation of magnetic stabilization in Perdew-Wang-type functionals.

We find that the bcc phase is mechanically unstable with respect to a tetragonal strain (space group $I4/mmm$) at pressures above approximately 100 GPa in both GGA and LSDA approximations (Fig. 3). At low pressure, GGA and LSDA correctly show mechanical stability of the bcc and fcc phases. Temperature-induced restabilization of the bcc phase at high pressure by anharmonic lattice modes is possible in principle but unlikely because of the magnitude of the instability in iron. The bcc structure is also highly unfavorable energetically relative to the close-packed structures at pressures comparable to those in the earth's inner core (Fig. 1). The energy difference between bcc and hcp (8000 K per atom)

exceeds even the highest estimates of the thermal energy available in the inner core.¹ Because of the energetic unfavorability and mechanical instability of bcc, it is highly unlikely that the inner core is composed of this phase, as has frequently been proposed.³¹

We have found exceptional agreement between first-principles calculations using the PW-II GGA functional and experiment over a nearly twofold range of compression. This represents the widest compression range over which theory and experiment have been successfully compared for a transition metal. The results are a substantial improvement over the LSDA and are in better agreement with data than those obtained with PW-I. We hope that the success of the PW-II functional for iron will stimulate further work on iron and other transition metals. The bcc phase is found to be energetically unfavorable and mechanically unstable at high pressures, making it a highly unlikely constituent of the earth's inner core.

This work supported by NSF (EAR-9305060). Work at NRL supported by the Office of Naval Research. Computations performed at the National Center for Supercomputer Applications and the Pittsburgh Supercomputer Center.

¹R. Jeanloz, *Ann. Rev. Earth Planet. Sci.* **18**, 357 (1990).

²K. C. Creager, *Nature (London)* **356**, 309 (1992); J. Tromp, *Nature (London)* **366**, 678 (1993).

³R. T. Merrill and M. W. McElhinny, *The Earth's Magnetic Field* (Academic, New York, 1983).

⁴Q. Williams *et al.*, *Science* **236**, 181 (1987).

⁵R. Boehler, *Nature (London)* **363**, 534 (1993).

⁶S. K. Saxena, G. Shen, and P. Lazor, *Science* **260**, 1312 (1993).

⁷J. M. Brown and R. G. McQueen, *J. Geophys. Res.* **91**, 7485 (1986); C. S. Yoo *et al.*, *Phys. Rev. Lett.* **70**, 3931 (1993).

⁸M. Körling and J. Häglund, *Phys. Rev. B* **45**, 13 293 (1992).

⁹C. S. Wang, B. M. Klein, and H. Krakauer, *Phys. Rev. Lett.* **54**, 1852 (1985).

¹⁰O. Gunnarsson and B. I. Lundqvist, *Phys. Rev. B* **13**, 4274 (1976).

¹¹D. C. Langreth and M. J. Mehl, *Phys. Rev. Lett.* **47**, 446 (1981); *Phys. Rev. B* **28**, 1809 (1983); **29**, 2310(E) (1984); C. D. Hu and D. C. Langreth, *Phys. Scr.* **32**, 391 (1985).

¹²J. P. Perdew and Y. Wang, *Phys. Rev. B* **33**, 8822 (1986); **40**, 3399(E) (1989); J. P. Perdew, *ibid.* **33**, 8822 (1986); **34**, 7406(E) (1986).

¹³J. P. Perdew *et al.*, *Phys. Rev. B* **46**, 6671 (1992).

¹⁴E. H. Lieb and S. Oxford, *Int. J. Quantum Chem.* **19**, 427 (1981).

¹⁵M. Levy, *Phys. Rev. A* **43**, 4637 (1991).

¹⁶P. Bagno, O. Jepsen, and O. Gunnarsson, *Phys. Rev. B* **40**, 1997 (1989).

¹⁷B. Barbiellini, E. G. Moroni, and T. Jarlborg, *J. Phys. Condens. Matter* **2**, 7597 (1990).

¹⁸T. C. Leung, C. T. Chan, and B. N. Harmon, *Phys. Rev. B* **44**, 2923 (1991).

¹⁹D. J. Singh, W. E. Pickett, and H. Krakauer, *Phys. Rev. B* **43**, 11 628 (1991).

²⁰C. Amador, W. R. L. Lambrecht, and B. Segall, *Phys. Rev. B* **46**, 1870 (1992).

²¹T. Asada and K. Terakura, *Phys. Rev. B* **46**, 13 599 (1992).

²²J. Häglund, *Phys. Rev. B* **47**, 566 (1993).

²³A. P. Jephcoat, H. K. Mao, and P. M. Bell, *J. Geophys. Res.* **91**, 4677 (1986).

²⁴H. K. Mao *et al.*, *J. Geophys. Res.* **95**, 21 737 (1990).

²⁵S. Wei and H. Krakauer, *Phys. Rev. Lett.* **55**, 1200 (1985).

²⁶U. von Barth and L. Hedin, *J. Phys. C* **5**, 1629 (1972).

²⁷D. Singh, *Phys. Rev. B* **43**, 6388 (1991).

²⁸A. Baldereschi, *Phys. Rev. B* **7**, 5212 (1973); D. J. Chadi and M. L. Cohen, *ibid.* **8**, 5747 (1973); H. J. Monkhorst and J. D. Pack, *ibid.* **13**, 5188 (1976).

²⁹B. Barbiellini, E. G. Moroni, and T. Jarlborg, *Helv. Phys. Acta* **64**, 164 (1991).

³⁰D. J. Singh and J. Ashkenazi, *Phys. Rev. B* **46**, 11 570 (1992).

³¹M. Ross, D. A. Young, and R. Grover, *J. Geophys. Res.* **95**, 21 713 (1990).

³²F. Birch, *J. Geophys. Res.* **57**, 227 (1952).

³³M. W. Guinan and D. N. Beshers, *J. Phys. Chem. Solids* **29**, 541 (1968).